

The Promise of Magnetic Resonance Imaging in Radiation Oncology Practice in the Management of Brain, Prostate, and GI Malignancies

Shashank Srinivasan, DNB¹; Archya Dasgupta, MD¹; Abhishek Chatterjee, MD¹; Akshay Baheti, MD²; Reena Engineer, MD, DNB¹; Tejal Gupta, MD, DNB¹; and Vedang Murthy, MD, DNB¹

Magnetic resonance imaging (MRI) has a key role to play at multiple steps of the radiotherapy (RT) treatment planning and delivery process. Development of high-precision RT techniques such as intensity-modulated RT, stereotactic ablative RT, and particle beam therapy has enabled oncologists to escalate RT dose to the target while restricting doses to organs at risk (OAR). MRI plays a critical role in target volume delineation in various disease sites, thus ensuring that these high-precision techniques can be safely implemented. Accurate identification of gross disease has also enabled selective dose escalation as a means to widen the therapeutic index. Morphological and functional MRI sequences have also facilitated an understanding of temporal changes in target volumes and OAR during a course of RT, allowing for midtreatment volumetric and biological adaptation. The latest advancement in linear accelerator technology has led to the incorporation of an MRI scanner in the treatment unit. MRI-guided RT provides the opportunity for MRI-only workflow along with online adaptation for either target or OAR or both. MRI plays a key role in post-treatment response evaluation and is an important tool for guiding decision making. In this review, we briefly discuss the RT-related applications of MRI in the management of brain, prostate, and GI malignancies.

JCO Global Oncol 8:e2100366. © 2022 by American Society of Clinical Oncology

Licensed under the Creative Commons Attribution 4.0 License 

INTRODUCTION

Magnetic resonance imaging (MRI) is an imaging modality on the basis of the principle of nuclear magnetic resonance. As hydrogen atoms constitute the major share of the human body, it enables the use of nuclear magnetic resonance for clinical imaging.¹ Since the first human MRI images were acquired in 1977, MRI has evolved rapidly with the development of relatively faster image acquisition, increase in magnetic field strength, and improved image processing techniques.^{2,3} The ability of noninvasive characterization of internal anatomy attributed to better soft-tissue clarity and the development of functional sequences to capture the internal physiology have facilitated numerous clinical applications of MRI. In clinical practice, MRI plays a pivotal role in diagnosis, disease staging, treatment planning, response monitoring, and surveillance after treatment completion.

Radiation oncology practice is deeply intertwined with imaging, primarily aiding in target volume and organs at risk (OAR) delineation and computing radiotherapy (RT) doses in the planning process (Fig 1). With the advancement and development of conformal and high-precision techniques such as

intensity-modulated radiotherapy, stereotactic radiosurgery, stereotactic body radiotherapy (SBRT), and particle beam therapy, the need for imaging modalities with better anatomical information has become essential.^{4,5} Insights from molecular imaging such as positron emission tomography (PET) and functional MRI have paved the way toward dose painting.⁶ Similarly, midtreatment volumetric and biological adaptation using morphological and functional MRI sequences accounting for changes to the target volumes and OAR can help improve the therapeutic ratio in the form of adaptive RT.⁷ Image-guided radiotherapy involving online imaging before treatment delivery has improved the precision and accuracy of treatment delivery.⁸ The traditional platforms for image-guided radiotherapy involve computed tomography (CT) built in the treatment unit. The integration of a compatible MRI scanner with a linear accelerator (linac) device has successfully led to an MR-linear accelerator (MR-Linac), which had been introduced in clinical practice, popularly known as MRI-guided radiotherapy (MRgRT).^{9,10} In this review, we briefly discuss the clinical applications of MRI in the management of brain, prostate, and GI malignancies from the perspective of radiation oncologists.

Author affiliations and support information (if applicable) appear at the end of this article.

Accepted on April 22, 2022 and published at ascopubs.org/journal/go on May 24, 2022; DOI <https://doi.org/10.1200/GO.21.00366>

CONTEXT

Key Objective

Magnetic resonance imaging (MRI) constitutes an integral role in contemporary oncology practice. This review was aimed at discussing radiotherapy (RT)-related applications of MRI in the context of brain, prostate, and GI malignancies.

Knowledge Generated

MRI plays a crucial role in decision making, RT planning and delivery, and response evaluation. MRI protocols including standardized sequences and slice thickness are required for target volume and organs at risk delineation for individual disease sites. The advent of MRI-linear accelerator (MR-Linac) provides opportunities for precise treatment delivery and real-time treatment adaptation, potentially improving therapeutic ratio. The merits of using MR-Linac are being investigated in ongoing clinical trials, with recent evidence suggesting reduction in acute toxicities with prostate stereotactic body radiotherapy delivered on MR-Linac.

Relevance

This review summarizes the current and expanding role of MRI in brain, prostate, and GI malignancies to allow optimum integration with RT practice.

ROLE OF MRI IN CONTEMPORARY RADIATION ONCOLOGY PRACTICE

CNS Malignancies

Rationale and parameters. MRI forms an indispensable part of the contemporary management of CNS tumors. The superior soft-tissue resolution, true multiplanar imaging capability, and the capacity for innate multiparametric functional imaging such as diffusion-weighted imaging (DWI), intravoxel incoherent motion, perfusion imaging, chemical exchange saturation transfer, and blood oxygenation level-dependent predicate a decisive advantage for MRI over all other forms of cross-sectional imaging in this regard. Typically, field strengths of 1.5-3T are used for routine imaging of CNS tumors, with no clear advantage of the higher field strength in clinical practice.¹¹ Imaging for

diagnosis and response assessment usually requires axial T1 (pregadolinium and postgadolinium), axial T2, and fluid-attenuated inversion recovery (FLAIR) sequences at minimum, with DWI, perfusion-weighted imaging, and MR spectroscopy assisting initial diagnosis and later distinction between tumor progression and pseudoprogression.^{12,13} Thin slice (1-2 mm width) volumetric sequences such as 3-dimensional fast spoilt gradient (3D FSPGR) and 3D FLAIR offer the advantages of rapid acquisition, good image reconstruction, and increased lesion detection rates, facilitating accurate delineation and ultra high-precision RT planning.¹⁴⁻¹⁶ Additional sequences such as steady-state free precession sequences (CISS/FIESTA sequence as used by vendors) and fat suppression sequences are often used in the delineation of skull base tumors or targets in close relation to the brain stem and cranial nerves

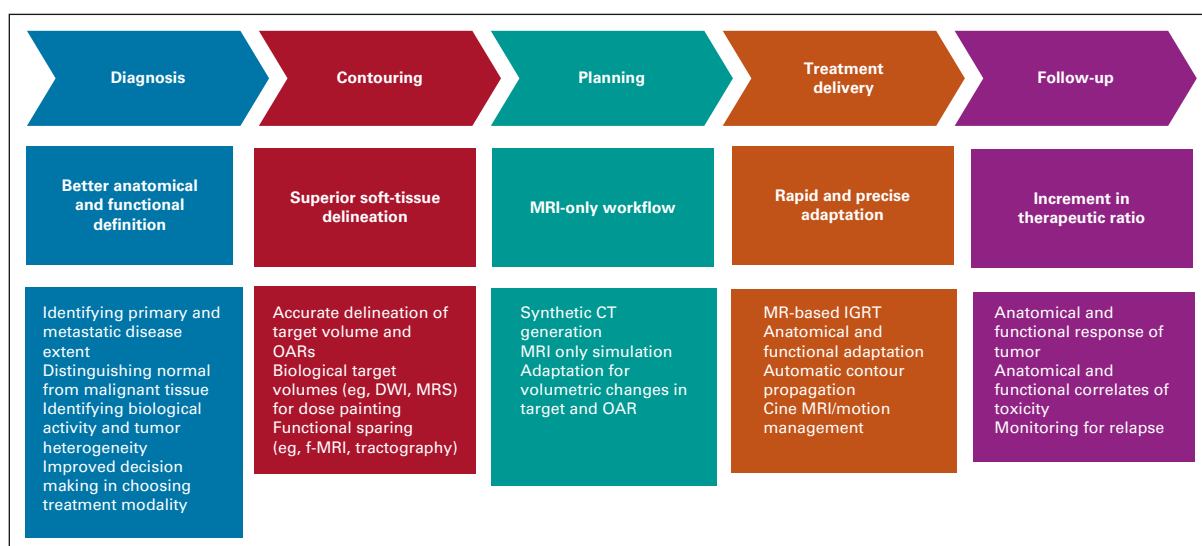


FIG 1. ROLE of MRI in radiation oncology workflow. CT, computed tomography; DWI, diffusion-weighted imaging; f-MRI, functional MRI; IGRT, image-guided radiotherapy; MRI, magnetic resonance imaging; MRS, spectroscopy; OAR, organs at risk.

(eg, chordoma, chondrosarcoma, meningioma, and schwannoma) because of anatomical clarity. Acquisition of thin-slice MRI sequences aids in accurate estimation of lesion size as higher slice width can lead to overestimation of the delineated structures because of interslice interpolation.¹⁷ Initial imaging should ideally be performed no later than 72 hours after surgery, else delayed by 2 weeks to avoid obfuscation of imaging findings by blood products and postoperative changes.¹² Imaging follow-up is usually performed at 4-6 weeks after RT conclusion, at completion of planned adjuvant therapy, and on clinical suspicion of progression or symptomatic worsening.¹⁸ Diffusion tensor imaging has proven beneficial in detecting radiation-induced demyelination and axonal degeneration,^{19,20} resulting in neurocognitive deterioration providing a window of changes before clinical manifestation and early interventions.

Clinical applications. MRI forms a crucial part of target delineation in primary and metastatic tumors in the CNS. Complementary sequences (T1 postcontrast MRI to delineate the enhancing residual and areas of leptomeningeal dissemination and T2/FLAIR to distinguish areas of infiltrative and nonenhancing tumors) are typically used for comprehensive delineation.^{21,22} MRI image fusion is typically achieved with a high degree of accuracy in the brain and is facilitated by the presence of rigid bony anatomical markers and limited movement of the brain within the calvarium. Rigid registration algorithms are usually sufficient for image fusion.^{23,24} The accuracy of image fusion is confirmed by matching standard anatomical references (clinoid processes, bony sella, tentorium cerebelli, and vertebral artery). The standard imaging protocols share the common caveat of inability to distinguish between infiltrative disease and vasogenic edema with reliability while delineating the clinical target volume. Additionally, contemporary recommendations on MRI anatomy facilitate delimitation of the clinical target volume with respect to anatomical barriers and provide useful adjuncts as practice shifts to MRI-based planning and delivery in the current decade²⁵ (Figs 2A and 2B).

The target volumes (postoperative cavity, surrounding infiltrative disease/vasogenic edema) in gliomas can undergo significant changes during the course of RT.²⁶ The dynamic changes offer the opportunity to modify elective target volumes as areas of putative tumor tissue reduce in responders to therapy. Similarly, special consideration is to be given to cystic tumors such as craniopharyngioma, wherein a significant proportion of patients have been reported to have changes in cyst dimensions requiring treatment modifications during a course of fractionated RT spanning over several weeks.²⁷ Automatic contour propagation facilitates real-time adaptation with accurate delineation in this regard.²⁸ The significant challenges in this regard remain the accurate determination of the shifting tumor-normal tissue interface on anatomic and functional imaging.

Limited evidence does suggest that it may be possible to distinguish the former from the latter through higher-order radiomic analysis, allowing one to potentially de-escalate RT in areas of response (reducing radiation necrosis and corticosteroid and bevacizumab usage rates) while intensifying therapy in voxels suggestive of radioresistance.²⁹ Although anatomical variations in the target and OARs are demonstrated during the course of fractionated RT, the clinical merits either in terms of improving disease control or reducing toxicities need to be proven from prospective clinical trials.

Functional MRI constitutes a profusion of sequences that allow for comprehensive biological assessment of a tumor and is emerging as a useful adjunct for optimizing treatment. It has long been known that metabolic abnormalities (increased choline, reduced n-acetyl aspartate, and increased lipid lactate) exist beyond the tumor.³⁰ In addition, areas with increased choline: n-acetyl aspartate ratios have also been found to correlate with adverse outcomes and are currently being targeted for dose escalation in clinical trials.³¹ Additional emerging areas for assessing tumor response include chemical exchange saturation transfer MRI, which can potentially detect both early response and tumor progression without the necessity for exogenous contrast.³² Noncontrast-based studies providing a combination of both diffusion and perfusion matrices such as intravoxel incoherent motion³³ provide another powerful tool for assessing response to treatment.³⁴ It is quite likely that such protocols in isolation or combination will provide opportunities for real-time biological adaptation in the setting of proliferation of MRI-based RT delivery systems with rapid onboard functional imaging capability. Table 1 shows selected studies for the role of MRI related to RT for brain tumors.

Prostate Cancer

Rationale and parameters. MRI is central to external beam radiotherapy planning for prostate cancer. Multiparametric MRI (mp-MRI) is the recommended technique in prostate cancer combining anatomical with functional imaging. This includes a high-resolution T2-weighted imaging (T2WI) with at least two functional MRI techniques. DWI, dynamic contrast-enhanced (DCE) perfusion imaging, and occasionally MR spectroscopy are commonly used. 3-T scanners are preferred to 1.5-T as they provide a higher signal to noise ratio allowing for better structural and functional details.³⁸ The study is performed on an external-phased array coil; using an endorectal coil does not offer significant benefit and may be avoided. Thin-slice (3 mm without interslice gap) T2W images with a small field of view (FOV) are used to depict prostate anatomy.³⁹ The high spatial resolution enables accurate assessment of extracapsular extension and seminal vesicle invasion. Addition of DWI aids in differentiating malignant from benign lesions with the former having restricted diffusion.⁴⁰

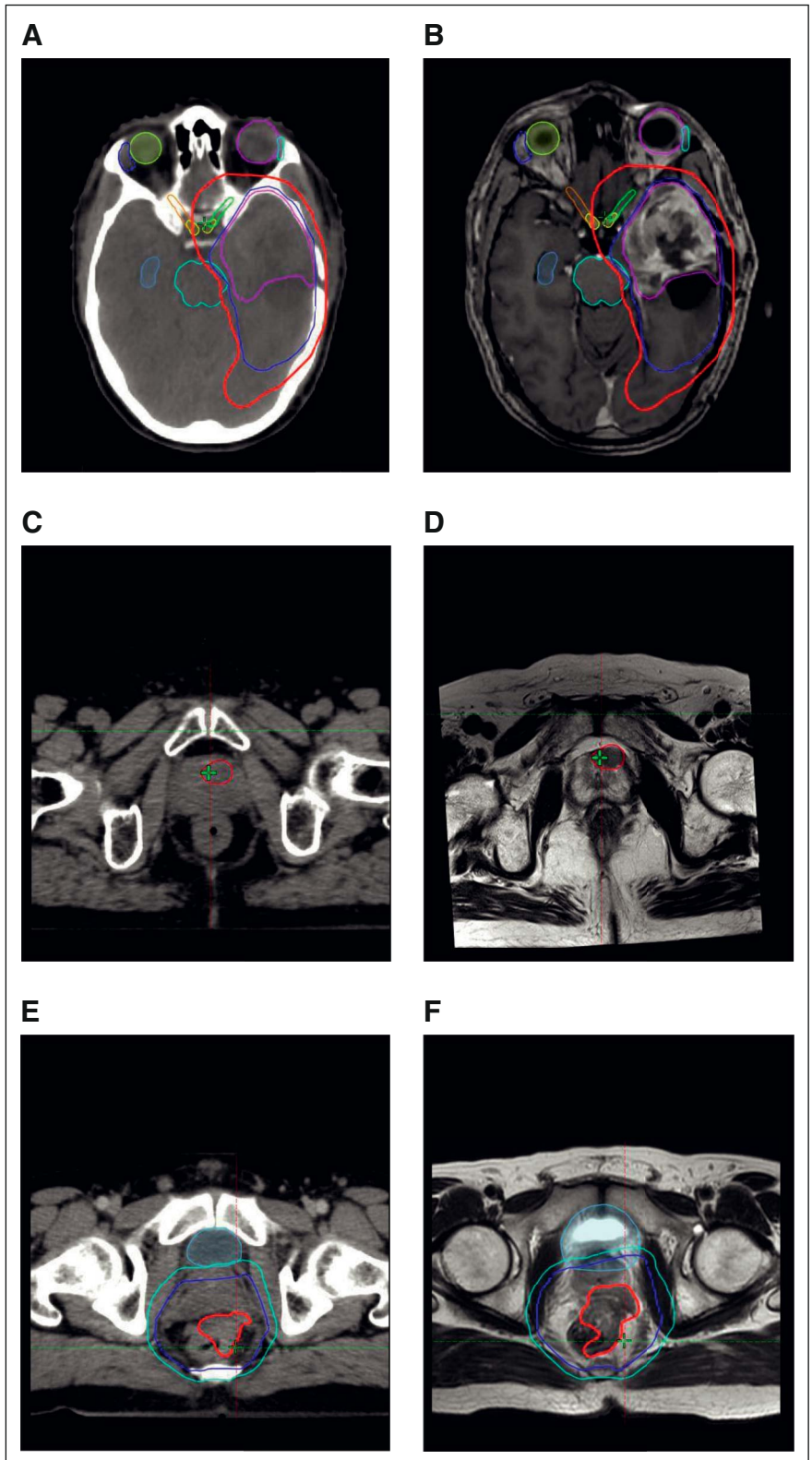


FIG 2. Composite diagram of CT and MRI used for radiation planning for brain, prostate, and GI malignancies. Representative CT and MRI scans acquired during radiation planning process. (A) Axial CT and (B) corresponding axial MRI T1-weighted contrast-enhanced sequence for a patient with glioblastoma. The target volumes are seen over the left temporal lobe: GTV (magenta), CTV (blue), and PTV (red). The extension of PTV in the basifrontal region was a result of expansion from extension of CTV in the superior slices (not seen in this image). (C) Axial CT and (D) corresponding axial T2W MRI for a patient with prostate cancer. Dominant intraprostatic lesion clearly visualized (in red) on the MRI, whereas it could not be discerned on the planning CT images, thus facilitating dose escalation to the DIL. (E) Axial CT and (F) corresponding axial T2W MRI for a patient with locally advanced rectal adenocarcinoma. Target volumes include GTV (red), CTV (purple), and PTV (light blue). The extension of the gross disease into the prostate could be accurately seen only on the MRI. CT, computed tomography; CTV, clinical target volume; DIL, dominant intraprostatic lesion; MRI, magnetic resonance imaging; PTV, planning target volume.

Clinical applications. MRI plays a pivotal role in target volume delineation in prostate RT. The apex and base of the prostate are often poorly visualized on CT. MRI helps to differentiate the prostatic apex from the genitourinary

diaphragm and the penile bulb and the base of the prostate from the bladder wall.

One of the biggest challenges for the use of MRI for volume delineation is the accuracy of CT and MRI coregistration as

TABLE 1. Selected Studies Showing the Clinical Application of MRI in CNS Tumors

Author, Year	Study Criteria (No. of patients)	Application	Comments
Thornton et al, ³⁵ 1992	GBM (60)—patients treated with CT-based planning with MRI (T1 plain, T1C, and T2) information integrated	Delineation	1. MRI markedly increased apparent tumor volume, as compared with CT Justifies the necessity of incorporating MRI into all contemporary conformal planning
Stall et al, ³⁶ 2010	GBM (40)—comparison of volumes drawn on T2 and FLAIR	Delineation	1. FLAIR CTVs and PTVs significantly larger than those on T2 2. Incorporation of FLAIR abnormality does not lead to significant OAR overdose 3. GTV at recurrence correlates best with FLAIR CTV Substantiates the usage of FLAIR sequences as an integral imaging sequence for planning in diffuse gliomas
Thrower et al, ¹⁷ 2021	Brain mets (28)—102 mets contoured on original images (1 mm) Images resampled to simulate acquisitions at 2- and 3-mm slice thickness Recontoured by experienced physicians	Delineation	Missed lesions: 1. 3% on 2 mm images 2. 13% on 3 mm images Increased size of contour 1. 11% larger on 2 mm images 2. 43% larger on 3 mm images 3. Underscores the need for thin slice imaging to allow for optimal delineation
Mehta et al, ³⁷ 2018	GBM (3)—0.35-T MRI/cobalt(Viewray)	Adaptation	1. General decrease in cavity measurements in all patients 2. One patient-transient increase followed by decrease Showcased potential for daily imaging and onboard adaptation of plan to improve tumor targeting and reduction of normal tissue irradiated
Lee et al, ²⁸ 2019	GBM (14)—MRIs performed at fractions 0, 10, 20, and 30 Three sets of contours: 1. Manual 2. Rigidly registered (static) 3. Semiautomatic propagation Compared using DSC and HD Dosimetric impact determined by comparing D0.03 cc	Adaptation	Using manual contours as reference, when compared with static contours, propagated contours have 1. Significantly higher DSC 2. Significantly lower HD 3. Significantly lower absolute difference in D0.03 cc Semiautomatic propagated contours have more accurate delineation and thereby facilitate more accurate OAR reporting
Stewart et al, ²⁶ 2021	GBM (61)— MRIs performed at fractions 0, 10, 20, and 30 Target dynamics were quantified by 1. Absolute volume (V) 2. Volume relative to Fx0 (V_{rel}) 3. Migration distance ($d_{migrate}$: the linear displacement of the GTV or CTV relative to Fx0)	Adaptation	1. GTV (CTV) migration distances were > 5 mm in 46% (54%) of patients at Fx10, 50% (58%) of patients at Fx20, and 52% (57%) of patients at P1M 2. 40% of patients exhibited a decreased GTV ($V_{rel} \leq 1$) with a $d_{migrate} > 5$ mm during chemoradiation therapy Clinically meaningful tumor dynamics encountered make a convincing case for daily MRI-guided RT and online plan adaptation

Abbreviations: CT, computed tomography; CTV, clinical target volume; DSC, dice similarity coefficient; FLAIR, fluid-attenuated inversion recovery; GBM, glioblastoma; GTV, gross tumor volume; HD, Hausdorff distance; mets, metastases; MRI, magnetic resonance imaging; OAR, organs at risk; P1M, post chemoradiation 1 month; PTV, planning target volume; RT, radiotherapy.

pelvic organs have nonrigid anatomy. The CT and T2W MRI images are fused using rigid automatic registration algorithm (on the basis of bony landmarks) and thereafter can be adjusted manually. For patients who have gold fiducial seeds implanted before the simulation scans, the images are aligned on the basis of the midpoint of the gold seeds. The prostate is then evaluated in all three planes to ensure precise anatomical superimposition. The presence of gold fiducial markers offers advantages for image coregistration as it overcomes the issue of accurately defining bony landmarks on MRI. Wegener et al⁴¹ showed that with the use of gold markers, the CT and MRI matching precision was within 2 mm.

Some of the issues precluding accurate CT-MRI coregistration are variations in rectal and bladder filling and patient position for the two scans with CT scan usually performed on a flat couch with knee support and the MRI being performed on a rounded table top unless using a dedicated MRI simulator. Chen et al⁴² showed that significant fusion uncertainties of > 4 mm were seen in 8.6% (anteroposterior direction) and 11.4% (superoinferior direction) of the patients with higher difference when scans were performed on different days. Patients with gold seed markers in situ had less prostate fusion uncertainties.

Prostate volume, as delineated on MRI, is nearly 30%-40% smaller than that delineated on CT with less interobserver variability.⁴³⁻⁴⁷ The maximum discrepancy in the two volumes is in the region of the prostatic apex and at the base of the seminal vesicles. Reduction in the target volumes potentially translates into better OAR sparing. Steenbakkers et al⁴⁸ showed that the rectal wall for CT-delineated prostate plans received 5.1 Gy higher equivalent uniform dose, and the penile bulb received 11.6 Gy higher mean dose than the MRI-delineated prostate plans. This also meant that allowing for the same rectal wall dose, the planning target volume (PTV) dose could be escalated from 78 Gy to 85 Gy using plans on the basis of MRI delineation of the prostate. Ali et al⁴⁹ compared intensity-modulated radiotherapy plans generated using CT-MRI delineation versus CT alone and found a statistically significant reduction in dose to the bladder and rectum with an approximately 22% reduction in Gr2 GU toxicity for CT-MRI patients, as compared with CT alone.

Patients with prostate cancer who develop local recurrence tend to do so at the site of the dominant intraprostatic lesion (DIL).⁵⁰ mp-MRI provides excellent visualization of the DIL and has allowed the escalation of dose to the DIL to > 90 Gy^{51,52} (Figs 2C and 2D). The FLAME trial randomly assigned patients with localized prostate cancer to either standard RT (77 Gy to the entire prostate) or an additional integrated focal boost to the DIL to a dose of upto 95 Gy. The dose-escalation arm showed a superior biochemical disease-free survival (92% v 85%, $P < .001$) at 5 years with no difference in overall survival or toxicity.⁵³ Most studies for DIL boost have used a combination of T2WI plus DCE plus

DWI for delineation of the DIL. However, recent studies have suggested that the actual DIL may correlate better with the volume delineated on Ga 68 prostate membrane-specific antigen PET-CT. Zamboglou et al⁵⁴ reported the combined use of prostate membrane-specific antigen PET CT and mp-MRI for the delineation of DIL and correlated it with the tumor control probability (TCP) on the basis of histology. On average, $86\% \pm 10\%$, $74\% \pm 17\%$, and $93\% \pm 5\%$ of GTV as seen on the histology specimen overlapped with PTV generated on PET, MRI, and combined PET/MRI, respectively. The plan generated using combined information from PET and MRI had significantly higher TCP values than either PET or MRI alone.

MRI as the sole imaging modality for RT treatment planning is gaining ground saving additional CT scan required for RT planning and eliminating the uncertainties from coregistration. As part of the MRI-only workflow, a pseudo-CT or synthetic CT is generated for dose computation. The methods for generating synthetic CT can be classified into voxel-based, atlas-based, and hybrid methods,⁵⁵ with expected dose differences performed on synthetic images compared with standard CT being within 1%.^{56,57} MRI-only workflow also enables automatic delineation of prostate and OARs which can be manually adjusted. Patient setup for treatment is achieved by matching synthetic DRRs with a success rate of > 90%^{58,59} with constraints in remaining 10% because of inability to accurately identify gold fiducial markers appearing as signal void. Other issues include artifacts generated by metallic implants,⁵⁹ large separation resulting in body contour reaching outside the FOV, and image distortion related to motion artifacts.

Interfraction and intrafraction variation of the prostate during RT has significant dosimetric and clinical implications. The use of MR-Linac can improve accuracy of delivery and combine it with real-time adaptive planning. Online matching of prostate using MRI is more accurate and thus can also be a factor in reducing PTV margins.⁶⁰ The use of cine-MRI during beam delivery affords the option to intervene in the event of extreme anatomical changes. Using motion monitoring and gating, it has been reported that 2D shifts during treatment are required in > 20% of all delivered fractions.⁶¹ Table 2 shows selected studies highlighting the role of MRI in various aspects of RT for prostate cancer.

Multiple prospective studies exploring the utility of MR-Linac for prostate RT are currently underway. Recently, the interim analysis from the phase III randomized MIRAGE study was presented⁶⁵ comparing SBRT for localized prostate cancer (40 Gy/5 fr) using CT versus MRI guidance. The primary end point was acute grade ≥ 2 GU toxicity within 90 days. One hundred patients were evaluated (51 CT and 49 MRI arm). MRI-guided SBRT had significantly lower acute grade ≥ 2 GU and GI toxicity (22.4% v 47.1%, $P = .01$ and 0 vs 13.7%, $P = .01$, respectively). Patient-reported outcome in the form of EPIC-26 bowel domain

TABLE 2. Selected Studies Showing the Clinical Application of MRI in Prostate Cancer

Author, Year	Study Criteria (No. of patients)	Application	Comments
Rasch et al, ⁴³ 1999	n = 18 Prostate delineated on CT and MRI for all patients	Delineation	1. The average ratio of volume delineated on CT v MRI was 1.4 Emphasizes the routine use of MRI along with CT data set for target volume delineation
Rischke et al, ⁶² 2013	n = 5 90 GTV data sets with DIL delineation on T2WI, DWI, and DCE by six observers	Target delineation for DIL	1. Excellent interobserver agreement based when DIL contoured on T2WI and DCE with lesser degree of difficulty of delineation as compared with DWI Shows feasibility of DIL boost using MRI
Gunnlaugsson et al, ⁶³ 2019	n = 7 CTV delineated on CT/MR and MR only 7-11 months apart	Target delineation in MRI only workflow (comparing MR/CT v MRI-only workflow)	1. 18% reduction in mean CTV volume in MRI-only workflow delineation Highlights the increased precision with MRI-only workflow as it overcomes CT/MRI coregistration issues
Tetar et al, ⁶¹ 2019	n = 140 700 fractions (SBRT) delivered using MRI only workflow with online plan adaptation	MRgRT-treatment and online adaptation	1. Plan reoptimized in 97% of fractions 2. All adapted treatment plans passed patient-specific QA 3. The average duration of an MRgRT fraction was 45 minutes Established feasibility of MR-Linac use in clinical practice
Bruynzeel et al, ⁶⁴ 2019	n = 104 SBRT 36.25 Gy/5 fr using MR-Linac (phase II), primary end point early toxicity	MRgRT-toxicity data	1. Maximum cumulative \geq Gr2 GU and GI toxicity was 23.8% and 5%, respectively, which peaked at last fraction and declined at 6 weeks follow-up 2. Corroborated by PROMs data First prospective study to report toxicity data for patients treated by MRgRT

Abbreviations: CT, computed tomography; CTV, clinical target volume; DCE, dynamic contrast enhanced; DIL, dominant intraprostatic lesion; DWI, diffusion-weighted imaging; Gr2, grade 2 toxicity; GTV, gross tumor volume; GU, genitourinary; MRgRT, MRI-guided radiotherapy; MRI, magnetic resonance imaging; MR-Linac, MR-linear accelerator; QA, quality assurance; PROM, patient-reported outcome measurement; SBRT, stereotactic body radiotherapy; T2WI, T2-weighted imaging.

scores was also in favor of the MRI-guided SBRT arm. Of note, the PTV margins used for MRI guidance were smaller than those for CT guidance (2 mm and 4 mm, respectively) and could have contributed to the large difference in the effect between the two arms.

GI Malignancies

Rationale and parameters. MRI has had a far-reaching impact in the management of GI malignancies right from staging, RT treatment planning, and execution to follow-up. MRI for rectal cancer should be performed using a 1.5-T or 3-T scanner with phased array coil positioned from the sacral promontory to 10 cm below the pubic symphysis.⁶⁶ The use of an endorectal coil is not beneficial.⁶⁷ The standard rectal MRI protocol includes 2D FSE T2-weighted non-fat-suppressed sequences. The sagittal series from one pelvic sidewall to another locates the tumor. Axial images are taken with a large FOV covering the entire pelvis and a smaller FOV with < 3 mm slice thickness axial and coronal to the long axis of the tumor. For low-lying rectal tumors, high-resolution coronal images are used to demonstrate levator muscles, sphincter complex, and intersphincteric plane. These sequences have high accuracy for identifying invasion of adjacent organs and mesorectal fascia and for extramural vascular invasion.⁶⁷

Traditionally, for liver lesions, multiphase CT or MRI is used for imaging. MRI has been shown to have higher sensitivity compared with CT scan for the diagnosis of hepatocellular

carcinoma, especially for lesions < 1 cm.⁶⁸ The minimum specifications for liver MRI include the use of a minimum 1.5-T scanner with phased array torso coil. The minimum sequences to be acquired are T2-weighted (with and without fat saturation), T1-weighted in- and out-of-phase images, dynamic postcontrast gadolinium T1-weighted gradient echo sequence (3D preferable), and preferably DWI. The dynamic sequences would include late arterial phase (30-35 seconds postcontrast), portal venous phase (60-70 seconds postcontrast), and delayed phase (3-5 minutes) with < 5 mm slice thickness.⁶⁹ Patients need to hold breath similarly for each sequence. The addition of DWI increases the detection rates, especially for smaller tumors.⁷⁰ There is also emerging use of hepatobiliary-specific contrast agents such as gadoxetate disodium, which is progressively transported into hepatocytes and excreted through the bile ducts.

Clinical applications. MRI is becoming a cornerstone in the RT planning process for upper abdominal tumors. Voroney et al compared MRI and CT-derived target volumes for liver tumors (primary and metastases) and found significant differences in the median percentage surface area difference. The median values for the percentage of surface area differing by 3 mm and 5 mm in spatial position between CT-GTV and MRI-GTV were 55% and 26%, respectively, with certain tumor foci visible only on MRI.⁷¹ Pech et al⁷² showed that the volume of liver metastases contoured using MRI was significantly larger than that on CT, with the

difference between the target volumes being 181% for T1w images, 178% for contrast-enhanced T1w, and 246% for T2w sequences.

MRI-based target volume delineation in rectal cancer has been studied in a limited number of patients, and it has been shown that the MRI-derived volume is smaller than CT with significant differences when anal canal and sigmoid are involved⁷³ (Figs 2E and 2F). Issues with CT and MRI coregistration owing to bladder filling and rectal distention at the time of the two scans preclude the routine use of MRI for external beam radiotherapy planning in rectal cancers. The best use of MRI for RT planning in rectal cancers may be for dose escalation wherein the T2 intermediate bright tumor can be accurately delineated and selectively boosted to a higher dose.⁷⁴

Managing motion of upper abdominal organs is a significant issue during RT planning and execution. Breathing-related motion artifacts during planning CT acquisition lead to incorrect target delineation, altered dosimetry, and eventually excessive PTV margins. Cine-MRI can be used to directly visualize the 3-dimensional tumor motion. Studies for liver motion using cine-MRI have demonstrated that four-dimensional CT scan underestimated motion while fluoroscopy overestimated motion relative to cine-MRI.⁷⁵ Pancreatic motion as assessed using cine MRI ranges from 6 to 34 mm, suggesting individualized PTV margins.⁷⁶

Table 3 summarizes selected studies highlighting the role of MRI in various aspects of RT for GI malignancies.

MR-guided RT is most suitable for sites where isodensity on CT does not allow discrimination of targets, especially if

TABLE 3. Selected Studies Showing the Clinical Application of MRI in GI Tumors

Author, Year	Study Criteria (No. of patients)	Application	Comments
Pech et al, ⁷² 2008	Liver mets (43 mets)—GTV delineated on CT and MRI for all patients	Target delineation	1. Tumor volume as contoured on MRI markedly increased over that contoured on CT Emphasizes the need for incorporating MRI as a complementary investigation for target volume delineation and planning in radiotherapy for upper abdominal tumors
Tan et al, ⁷³ 2010	Ca rectum (15) T3 rectal cancer—GTV drawn on planning CT and MRI performed in treatment position	Target delineation	1. The mean CT-GTV/MR-GTV ratio was 1.2 2. Discrepancy between the two contours was seen when there was invasion of sigmoid and anal canal Explores the role of simulation MRI for rectal cancer
Heerkens et al, ⁷⁶ 2014	Ca pancreas (15)—two cine MRIs of 60 s duration performed MOSSE adaptive correlation filter used to quantify tumor motion in AP, lateral, and CC directions	Motion management	1. Maximum motion in CC direction, average 15 mm (6-34 mm), AP direction average 5 mm, lateral average 3 mm Study brings to light the role of MRI in individualization of PTV margins and active motion management strategies
Henke et al, ⁷⁷ 2017	Oligometastatic or unresectable primary liver (10) or nonliver (10) upper abdominal malignancies (phase I study)—underwent SMART-50 Gy/5 fr	MRgRT—treatment and online adaptation	1. Daily adapted plan deemed to be superior to initial plan for 83.5% (81 of 97) fractions 2. 100% of nonliver fractions were adapted 3. 61 of 81 (75%) fractions adapted for reversing OAR constraint violation 4. 20 fractions adapted to increase PTV dose coverage 5. Median on-table time: 79 minutes 6. Local PFS 95% and 89.1% at 3 and 6 months, respectively 7. No Gr3 toxicity at 6 months First prospective clinical study of SMART
de Jong et al, ⁷⁸ 2015	Meta-analysis—included studies (n = 46 studies/ 2,224 patients) evaluating the performance of MRI, CT, and endoscopic ultrasound (ability to detect complete response) for restaging of locally advanced rectal cancer (T3-T4 and/or N1) after neoadjuvant therapy	Post-treatment response evaluation (as part of watch and wait strategy for organ preservation)	1. Pooled accuracy: 75% 2. Sensitivity: 95% 3. Specificity: 31% 4. Positive predictive value: 83% 5. Negative predictive values: 47% Findings suggest that MRI may be more useful to rule out complete response rather than to confirm it

Abbreviations: AP, anteroposterior; CC, craniocaudal; CT, computed tomography; MRgRT, MRI-guided radiotherapy; mets, metastases; MOOSE, Minimum Output Sum of Squared Error; MRI, magnetic resonance imaging; OAR, organs at risk; PFS, progression-free survival; PTV, planning target volume; RT, radiotherapy; SMART, stereotactic MR-guided online adaptive RT.

TABLE 4. Selected Ongoing Studies on MR-Linac in Brain Tumors, Prostate Cancer, and GI Cancers

Study (country)	Study Design	Target Accrual	Study Population	Intervention	Primary End Point	Estimated Year of Completion
Brain tumors						
Unity-Based MR-Linac Guided Adaptive Radiotherapy for High Grade Glioma (UNITED) NCT04726397 (Canada)	Phase II, single arm	40	GBM receiving RT in 15 or 30# with or without temozolamide, expected survival > 12 weeks and maximum final planning volume < 150 cm ³	Reduced (5 mm) CTV margin with weekly adaptive RT on MR-Linac	Marginal failure within 1 year from radiation	2024
MR-Linac Guided Adaptive FSRT for Brain Metastases From Non-small Cell Lung Cancer (NSCLC) NCT04946019 (China)	Phase II, single arm	55	Histologically/cytologically confirmed NSCLC with 1-10 brain metastases on CEMRI	FSRT to brain metastases—30 Gy/5 fr on MR-Linac	1 year intracranial progression-free survival	2023
Prostate cancer						
Five or Two MRI-Guided Adaptive Radiotherapy Treatments for Prostate Cancer (FORT) NCT04984343 (USA)	Phase II, randomized	136	Low- and intermediate-risk prostate cancer, IPSS < 18	1:1 random assignment to either 37.5 Gy/5 fr (alternate days) or 25 Gy/2 fr (at least 72 hours apart) with or without SIB to prostate with or without seminal vesicles	Change in the number of patient-reported GI symptoms using the EPIC at 2 years after treatment completion	2027
Hypofractionated Expedited Radiotherapy for Men With localisEd proState Cancer (HERMES) NCT04595019 (UK)	Phase II, randomized	46	Prostatic adenocarcinoma with Gleason's score 3 + 4 or 4 + 3, initial PSA < 25 ng/mL, MRI stage T3a or less	36.25 Gy in 5 fractions (boost to 40 Gy to tumor/prostate CTV) over 10 days v 24 Gy in 2 fractions (boost to 27 Gy to tumor/prostate CTV) over 8 days	GU toxicity at 12 months	2028
MIRAGE Study NCT04384770 (USA)	Phase III, randomized	300	Histologically confirmed clinically localized prostatic adenocarcinoma	5 fractions of CT-guided SBRT over 14 days v 5 fractions of MRI-guided SBRT over 14 days	Incidence of acute grade ≥ 2 GU physician-reported toxicity	2027
GI cancers						
Stereotactic MRI-guided on-table Adaptive Radiation Therapy (SMART) for Locally Advanced Pancreatic Cancer NCT03621644 (USA and Israel)	Phase II, single arm	133	Locally advanced pancreatic cancer considered to be borderline resectable or unresectable having received at least 3 months of systemic therapy	50 Gy/5 fr with MRI image guidance and online adaptive RT delivered at least twice a week	GI toxicity	2026

Abbreviations: CEMRI, contrast-enhanced magnetic resonance imaging; CT, computed tomography; CTV, clinical target volume; EPIC, Expanded Prostate Cancer Index Composite; FSRT, fractionated stereotactic radiotherapy; GBM, glioblastoma; GU, genitourinary; IPSS, international prostate symptom score; MRI, magnetic resonance imaging; MR-Linac, MR-linear accelerator; NSCLC, non-small-cell lung cancer; PSA, prostate-specific antigen; RT, radiotherapy; SBRT, stereotactic body radiotherapy; SIB, simultaneous integrated boost.

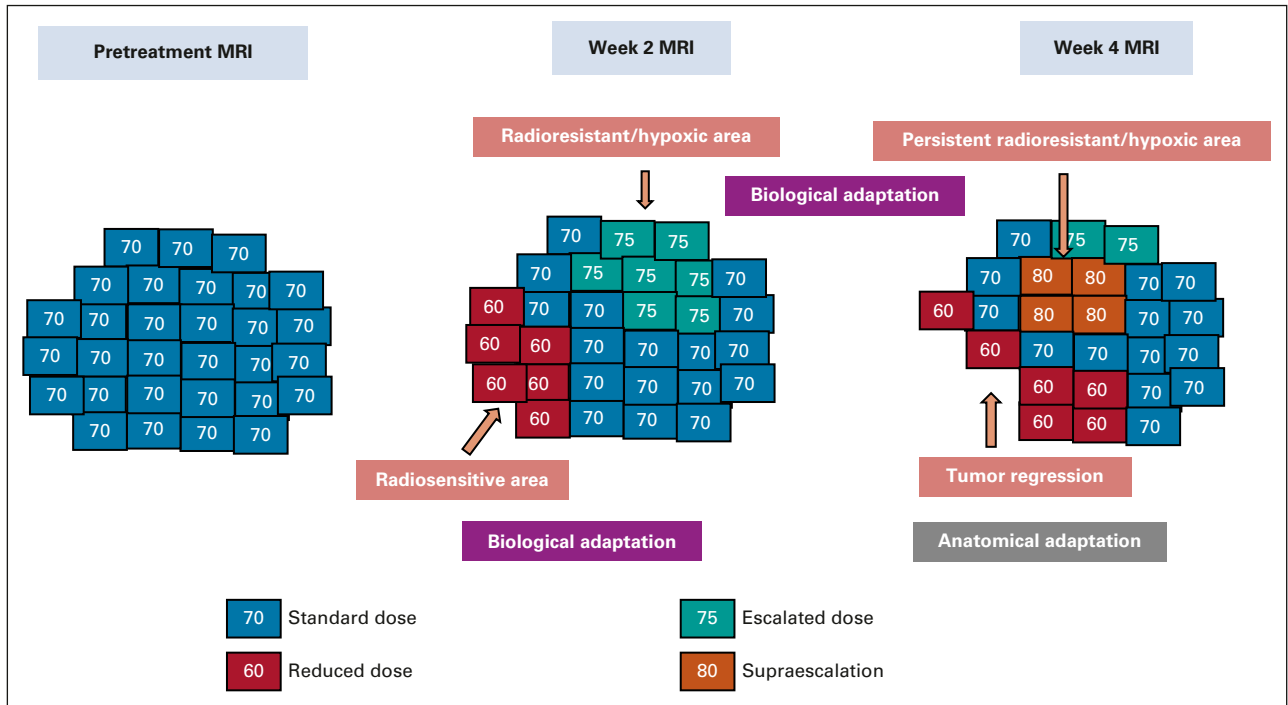


FIG 3. Schematic workflow for potential MRI-guided adaptive radiotherapy undertaken in a course of fractionated RT. MRI is performed at week 2 and week 4 during radiation. Anatomical adaptation is undertaken for morphological changes as detected on midtreatment MRI for target volumes and organs at risk. Biological adaptation with different dose levels is performed on the basis of findings from functional MRI, with areas of refractory disease escalated to a higher dose and areas with response de-escalated to a relatively lower dose level. MRI, magnetic resonance imaging; RT, radiotherapy.

mobile. This makes the upper abdomen an ideal candidate for the application of this modality, considering the growing role of SBRT for primary or metastatic liver tumors and pancreatic cancers to improve therapeutic ratio. A panel of radiation oncologists and radiologists with experience in MRgRT have published an atlas for OAR contouring of upper abdomen.⁷⁹ Peristalsis-related motion artifacts create difficulties for delineation in MR online workflow. However, drinking a glass of water shortly before the treatment fraction may help in visualizing structures, and antiperistaltic agents may reduce motion artifacts. Continuous real-time 2D cine-MRI is used to monitor target motion, thus obviating the need for implanting fiducial markers.⁸⁰ Changes in stomach filling and bowel distention in close proximity to targets call for online adaptation, especially for peripheral liver tumors and pancreatic lesions. There are two kinds of adaptive workflows: adapt to shape and adapt to position. Adapt to shape entails an adaptation of structures as seen on the day of treatment, whereas adapt to position refers to an isocenter shift because of the inability to shift the couch on the 1.5-T MR-Linac. Henke et al demonstrated the use of MRgART in their study of SBRT (50 Gy/5 fr) for metastases or unresectable abdominal tumors, wherein all constraints were met on initial radiation planning. However, for 81 of the 97 fractions, a daily adapted plan was deemed superior. Three quarters of the plans were adapted because of violation of an OAR constraint while the rest were performed to improve

target coverage. No \geq grade 3 toxicities were observed in the 15-month follow-up period.⁷⁷

MRI in conjunction with sigmoidoscopy for response evaluation after neoadjuvant chemoradiation in rectal cancers has heralded the wait and watch policy for patients with complete clinical response.^{81,82}

Table 4 summarizes selected ongoing studies on MR-Linac for brain, prostate, and GI malignancies.

FUTURE DIRECTIONS

The field of medical imaging and MRI is undergoing continuous refinements with contributions from physics, computer science, and related disciplines. Ultra high-field MRI systems using 7T have been introduced in clinical practice, and 10.5T MRI has been tested in humans recently to generate better structural and functional information from enhanced signal-to-noise and contrast-to-noise ratios.^{83,84} The contribution of artificial intelligence in quantitative analysis of medical imaging is an active area of research and is more popularly known as radiomics.⁸⁵ With MRI used in multiple steps of radiation oncology practice, radiomic analysis is expected to have a significant impact in the future to lead the way toward personalized radiation therapy.^{85,86} One of the major advances in the recent era in the therapeutic delivery of RT has been the introduction of MR-Linac in clinical practice. As described in previous

sections, the clinical application of MRgRT is still in its infancy, with two MR-Linacs introduced for patient treatment in the past 5 years. Generation of TCP and normal tissue complication probability models from daily MRgRT along with rapid contour propagation and plan optimization algorithms provide the window for real-time treatment adaptation as well as dose modification (escalation/de-escalation) for target and OARs^{87,88} (Fig 3). With ongoing conceptual refinements and applications, improving the precision of treatment delivery and better provision of adaptive RT, the actual clinical merits in toxicity reduction and/or better control rates need to be solicited in the future, compared with the available linac-based RT. Inspired by the IDEAL (Idea, Development, Exploration, Assessment, and Long-term evaluation) recommendations as described for the surgical development process,⁸⁹ the concept of R-IDEAL framework has been introduced for radiation oncology innovations.⁹⁰ Given the higher cost of the commercially available MR-Linacs compared with standard linear accelerators, it will be necessary to critically analyze the forthcoming evidence in the context of cost-benefit analysis, which is included in stage 3 of the R-IDEAL framework. The MR-Linac platform entails higher time on couch for the patient and demands increased human resources with the involvement of therapists, physicists, and oncologists. With artificial intelligence-based algorithms, fast

and robust real-time optimization procedures, modifications of contour, and planning can potentially make the adaptive workflow more efficient and less time-consuming. Further technological advances in the accelerator device of the MR-Linac with the ability to deliver higher-energy beams, thin-width microleaf collimators are desired in the future to improve radiation conformality. Finally, MRI provides opportunities for delivery of anticancer therapies such as MR-guided focused ultrasound, which can be used to induce hyperthermia, temporary opening of the blood-brain barrier, triggering drug delivery, and microbubble (ultrasound contrast) stimulation as radiosensitizers.⁹¹⁻⁹⁴

In conclusion, the contemporary practice of radiation oncology involves MRI in multiple instances including diagnosis, treatment planning, treatment delivery, midtreatment adaptation, response assessment, and surveillance. MR-Linac has been introduced in clinical practice recently is promising for real-time adaptation, improving the therapeutic ratio, although future clinical studies are warranted to establish the clinical advantages. Further developments in functional imaging sequences and quantitative imaging analysis incorporating artificial intelligence strategies are expected to have significant contributions in the future to pave the way toward precision oncology.

AFFILIATIONS

¹Department of Radiation Oncology, Tata Memorial Centre, Homi Bhabha National Institute, Mumbai, India

²Department of Radiodiagnosis, Tata Memorial Centre, Homi Bhabha National Institute, Mumbai, India

CORRESPONDING AUTHOR

Vedang Murthy, MD, DNB, Department of Radiation Oncology, Tata Memorial Hospital and Advanced Centre for Treatment, Research and Education in Cancer (ACTREC), Tata Memorial Centre, Dr E. Borges Rd, Parel, Mumbai 400012, India; e-mail: vmurthy@actrec.gov.in.

AUTHOR CONTRIBUTIONS

Conception and design: Shashank Srinivasan, Archya Dasgupta, Akshay Baheti, Tejal Gupta, Vedang Murthy

Provision of study materials or patients: Shashank Srinivasan, Archya Dasgupta, Vedang Murthy

Collection and assembly of data: Shashank Srinivasan, Archya Dasgupta, Abhishek Chatterjee, Akshay Baheti, Vedang Murthy

Data analysis and interpretation: Shashank Srinivasan, Akshay Baheti, Reena Engineer, Vedang Murthy

Manuscript writing: All authors

Final approval of manuscript: All authors

Accountable for all aspects of the work: All authors

AUTHORS' DISCLOSURES OF POTENTIAL CONFLICTS OF INTEREST

The following represents disclosure information provided by authors of this manuscript. All relationships are considered compensated unless otherwise noted. Relationships are self-held unless noted. I = Immediate Family Member, Inst = My Institution. Relationships may not relate to the subject matter of this manuscript. For more information about ASCO's conflict of interest policy, please refer to www.asco.org/rwc or ascopubs.org/go/authors/author-center.

Open Payments is a public database containing information reported by companies about payments made to US-licensed physicians ([Open Payments](http://OpenPayments)).

Shashank Srinivasan

Employment: GlaxoSmithKline

No other potential conflicts of interest were reported.

REFERENCES

- Pooley RA: AAPM/RSNA physics tutorial for residents: Fundamental physics of MR imaging. *Radiographics* 25:1087-1099, 2005
- Edelman RR: The history of MR imaging as seen through the pages of radiology. *Radiology* 273:S181-S200, 2014 (2 suppl)
- Plewes DB, Kucharczyk W: Physics of MRI: A primer. *J Magn Reson Imaging* 35:1038-1054, 2012
- Garibaldi C, Jereczek-Fossa BA, Marvaso G, et al: Recent advances in radiation oncology. *Ecancermedalscience* 11:785, 2017
- FitzGerald TJ, Rosen MA, Bishop-Jodoin M: The influence of imaging in the modern practice of radiation oncology. *Int J Radiat Oncol Biol Phys* 102:680-682, 2018
- Bentzen SM, Gregoire V: Molecular imaging-based dose painting: A novel paradigm for radiation therapy prescription. *Semin Radiat Oncol* 21:101-110, 2011

7. Keall P, Poulsen P, Booth JT: See, think, and act: Real-time adaptive radiotherapy. *Semin Radiat Oncol* 29:228-235, 2019
8. Jaffray DA: Image-guided radiotherapy: From current concept to future perspectives. *Nat Rev Clin Oncol* 9:688-699, 2012
9. Corradini S, Alongi F, Andratschke N, et al: MR-guidance in clinical reality: Current treatment challenges and future perspectives. *Radiat Oncol* 14:92, 2019
10. Hall WA, Paulson ES, van der Heide UA, et al: The transformation of radiation oncology using real-time magnetic resonance guidance: A review. *Eur J Cancer* 122:42-52, 2019
11. Tselikas L, Souillard-Scemama R, Naggara O, et al: Imaging of gliomas at 1.5 and 3 Tesla—A comparative study. *Neuro-Oncol* 17:895-900, 2015
12. Wen PY, Macdonald DR, Reardon DA, et al: Updated response assessment criteria for high-grade gliomas: Response assessment in neuro-oncology working group. *J Clin Oncol* 28:1963-1972, 2010
13. Lundy P, Domino J, Ryken T, et al: The role of imaging for the management of newly diagnosed glioblastoma in adults: A systematic review and evidence-based clinical practice guideline update. *J Neurooncol* 150:95-120, 2020
14. Metcalfe P, Liney GP, Holloway L, et al: The potential for an enhanced role for MRI in radiation-therapy treatment planning. *Technol Cancer Res Treat* 12:429-446, 2013
15. Tome WA, Mehta MP, Meeks SL, et al: Fractionated stereotactic radiotherapy: A short review. *Technol Cancer Res Treat* 1:153-172, 2002
16. Chagla GH, Busse RF, Sydnor R, et al: Three-dimensional fluid attenuated inversion recovery imaging with isotropic resolution and nonselective adiabatic inversion provides improved three-dimensional visualization and cerebrospinal fluid suppression compared to two-dimensional flair at 3 Tesla. *Invest Radiol* 43:547-551, 2008
17. Thrower SL, Al Feghali KA, Luo D, et al: The effect of slice thickness on contours of brain metastases for stereotactic radiosurgery. *Adv Radiat Oncol* 6:100708, 2021
18. Weller M, van den Bent M, Tonn JC, et al: European Association for Neuro-Oncology (EANO) guideline on the diagnosis and treatment of adult astrocytic and oligodendroglial gliomas. *Lancet Oncol* 18:e315-29, 2017
19. Mabbott DJ, Noseworthy MD, Bouffet E, et al: Diffusion tensor imaging of white matter after cranial radiation in children for medulloblastoma: Correlation with IQ. *Neuro Oncol* 8:244-252, 2006
20. Chapman CH, Zhu T, Nazem-Zadeh M, et al: Diffusion tensor imaging predicts cognitive function change following partial brain radiotherapy for low-grade and benign tumors. *Radiother Oncol* 120:234-240, 2016
21. Kruser TJ, Bosch WR, Badiyan SN, et al: NRG brain tumor specialists consensus guidelines for glioblastoma contouring. *J Neurooncol* 143:157-166, 2019
22. Niyazi M, Brada M, Chalmers AJ, et al: ESTRO-ACROP guideline “target delineation of glioblastomas.” *Radiother Oncol* 118:35-42, 2016
23. Iqbal K, Saima A, Aqeel M, et al: Brain gliomas CT-MRI image fusion for accurate delineation of gross tumor volume in three dimensional conformal radiation therapy. *OMICS J Radiol* 4, 2015
24. Guo L, Shen S, Harris E, et al: A tri-modality image fusion method for target delineation of brain tumors in radiotherapy. *PLoS One* 9:e112187, 2014
25. Tseng C-L, Stewart J, Whitfield G, et al: Glioma consensus contouring recommendations from a MR-Linac International Consortium Research Group and evaluation of a CT-MRI and MRI-only workflow. *J Neurooncol* 149:305-314, 2020
26. Stewart J, Sahgal A, Lee Y, et al: Quantitating interfraction target dynamics during concurrent chemoradiation for glioblastoma: A prospective serial imaging study. *Int J Radiat Oncol Biol Phys* 109:736-746, 2021
27. Winkfield KM, Linsenmeier C, Yock TI, et al: Surveillance of craniopharyngioma cyst growth in children treated with proton radiotherapy. *Int J Radiat Oncol Biol Phys* 73:716-721, 2009
28. Lee S, Stewart J, Lee Y, et al: Improved dosimetric accuracy with semi-automatic contour propagation of organs-at-risk in glioblastoma patients undergoing chemoradiation. *J Appl Clin Med Phys* 20:45-53, 2019
29. Dasgupta A, Geraghty B, Maralani PJ, et al: Quantitative mapping of individual voxels in the peritumoral region of IDH-wildtype glioblastoma to distinguish between tumor infiltration and edema. *J Neurooncol* 153:251-261, 2021
30. Chaumeil MM, Lupo JM, Ronen SM: Magnetic resonance (MR) metabolic imaging in glioma. *Brain Pathol* 25:769-780, 2015
31. Laprie A, Ken S, Filleron T, et al: Dose-painting multicenter phase III trial in newly diagnosed glioblastoma: The SPECTRO-GLIO trial comparing arm A standard radiochemotherapy to arm B radiochemotherapy with simultaneous integrated boost guided by MR spectroscopic imaging. *BMC Cancer* 19:167, 2019
32. Chan RW, Chen H, Myrehaug S, et al: Quantitative CEST and MT at 1.5T for monitoring treatment response in glioblastoma: Early and late tumor progression during chemoradiation. *J Neurooncol* 151:267-278, 2021
33. Le Bihan D, Breton E, Lallemand D, et al: Separation of diffusion and perfusion in intravoxel incoherent motion MR imaging. *Radiology* 168:497-505, 1988
34. Liu Z-C, Yan L-F, Hu Y-C, et al: Combination of IVIM-DWI and 3D-ASL for differentiating true progression from pseudoprogression of glioblastoma multiforme after concurrent chemoradiotherapy: Study protocol of a prospective diagnostic trial. *BMC Med Imaging* 17:10, 2017
35. Thornton AF, Sandler HM, Ten Haken RK, et al: The clinical utility of magnetic resonance imaging in 3-dimensional treatment planning of brain neoplasms. *Int J Radiat Oncol Biol Phys* 24:767-775, 1992
36. Stall B, Zach L, Ning H, et al: Comparison of T2 and FLAIR imaging for target delineation in high grade gliomas. *Radiat Oncol* 5:5, 2010
37. Mehta S, Gajjar SR, Padgett KR, et al: Daily tracking of glioblastoma resection cavity, cerebral edema, and tumor volume with MRI-guided radiation therapy. *Cureus* 10:e2346, 2018
38. Rouvière O, Hartman RP, Lyonnet D: Prostate MR imaging at high-field strength: Evolution or revolution? *Eur Radiol* 16:276-284, 2006
39. Hoeks CMA, Barentsz JO, Hambrock T, et al: Prostate cancer: Multiparametric MR imaging for detection, localization, and staging. *Radiology* 261:46-66, 2011
40. Hegde JV, Mulhern RV, Panych LP, et al: Multiparametric MRI of prostate cancer: An update on state-of-the-art techniques and their performance in detecting and localizing prostate cancer. *J Magn Reson Imaging* 37:1035-1054, 2013
41. Wegener D, Zips D, Thorwarth D, et al: Precision of T2 TSE MRI-CT-image fusions based on gold fiducials and repetitive T2 TSE MRI-MRI-fusions for adaptive IGRT of prostate cancer by using phantom and patient data. *Acta Oncol* 58:88-94, 2019
42. Chen X, Xue J, Chen L, et al: CT-MRI fusion uncertainty in prostate treatment planning for different image guidance techniques. *Int J Radiat Oncol* 87:S718, 2013
43. Rasch C, Barillot I, Remeijer P, et al: Definition of the prostate in CT and MRI: A multi-observer study. *Int J Radiat Oncol Biol Phys* 43:57-66, 1999
44. Roach M, Faillace-Akazawa P, Malfatti C, et al: Prostate volumes defined by magnetic resonance imaging and computerized tomographic scans for three-dimensional conformal radiotherapy. *Int J Radiat Oncol Biol Phys* 35:1011-1018, 1996
45. Sannazzari GL, Ragona R, Ruo Redda MG, et al: CT-MRI image fusion for delineation of volumes in three-dimensional conformal radiation therapy in the treatment of localized prostate cancer. *Br J Radiol* 75:603-607, 2002
46. Hentschel B, Oehler W, Strauss D, et al: Definition of the CTV prostate in CT and MRI by using CT-MRI image fusion in IMRT planning for prostate cancer. *Strahlenther Onkol* 187:183-190, 2011

47. Pathmanathan AU, McNair HA, Schmidt MA, et al: Comparison of prostate delineation on multimodality imaging for MR-guided radiotherapy. *Br J Radiol* 92:20180948, 2019
48. Steenbakkers RJHM, Deurloo KEI, Nowak PJCM, et al: Reduction of dose delivered to the rectum and bulb of the penis using MRI delineation for radiotherapy of the prostate. *Int J Radiat Oncol Biol Phys* 57:1269-1279, 2003
49. Ali AN, Rossi PJ, Godette KD, et al: Impact of magnetic resonance imaging on computed tomography-based treatment planning and acute toxicity for prostate cancer patients treated with intensity modulated radiation therapy. *Pract Radiat Oncol* 3:e1-e9, 2013
50. Cellini N, Morganti AG, Mattiucci GC, et al: Analysis of intraprostatic failures in patients treated with hormonal therapy and radiotherapy: Implications for conformal therapy planning. *Int J Radiat Oncol Biol Phys* 53:595-599, 2002
51. Feutren T, Herrera FG: Prostate irradiation with focal dose escalation to the intraprostatic dominant nodule: A systematic review. *Prostate Int* 6:75-87, 2018
52. Pickett B, Vigneault E, Kurhanewicz J, et al: Static field intensity modulation to treat a dominant intra-prostatic lesion to 90 Gy compared to seven field 3-dimensional radiotherapy. *Int J Radiat Oncol Biol Phys* 44:921-929, 1999
53. Kerkmeijer LGW, Groen VH, Pos FJ, et al: Focal boost to the intraprostatic tumor in external beam radiotherapy for patients with localized prostate cancer: Results from the FLAME randomized phase III trial. *J Clin Oncol* 39:787-796, 2021
54. Zamboglou C, Thomann B, Koubar K, et al: Focal dose escalation for prostate cancer using 68Ga-HBED-CC PSMA PET/CT and MRI: A planning study based on histology reference. *Radiat Oncol* 13:81, 2018
55. Owrangi AM, Greer PB, Glide-Hurst CK: MRI-only treatment planning: Benefits and challenges. *Phys Med Biol* 63:05TR01, 2018
56. Dowling JA, Lambert J, Parker J, et al: An atlas-based electron density mapping method for magnetic resonance imaging (MRI)-alone treatment planning and adaptive MRI-based prostate radiation therapy. *Int J Radiat Oncol Biol Phys* 83:e5-e11, 2012
57. Korhonen J, Kapanen M, Keyriläinen J, et al: A dual model HU conversion from MRI intensity values within and outside of bone segment for MRI-based radiotherapy treatment planning of prostate cancer: HU conversion from MRI data. *Med Phys* 41:011704, 2013
58. Tyagi N, Zelefsky MJ, Wibmer A, et al: Clinical experience and workflow challenges with magnetic resonance-only radiation therapy simulation and planning for prostate cancer. *Phys Imaging Radiat Oncol* 16:43-49, 2020
59. Tenhunen M, Korhonen J, Kapanen M, et al: MRI-only based radiation therapy of prostate cancer: Workflow and early clinical experience. *Acta Oncol* 57:902-907, 2018
60. Murray J, Tree AC: Prostate cancer—Advantages and disadvantages of MR-guided RT. *Clin Transl Radiat Oncol* 18:68-73, 2019
61. Tatar SU, Bruynzeel AME, Lagerwaard FJ, et al: Clinical implementation of magnetic resonance imaging guided adaptive radiotherapy for localized prostate cancer. *Phys Imaging Radiat Oncol* 9:69-76, 2019
62. Rischke HC, Nestle U, Fechter T, et al: 3 Tesla multiparametric MRI for GTV-definition of dominant intraprostatic lesions in patients with prostate cancer—An interobserver variability study. *Radiat Oncol* 8:183, 2013
63. Gunnlaugsson A, Persson E, Gustafsson C, et al: Target definition in radiotherapy of prostate cancer using magnetic resonance imaging only workflow. *Phys Imaging Radiat Oncol* 9:89-91, 2019
64. Bruynzeel AME, Tatar SU, Oei SS, et al: A prospective single-arm phase 2 study of stereotactic magnetic resonance guided adaptive radiation therapy for prostate cancer: Early toxicity results. *Int J Radiat Oncol Biol Phys* 105:1086-1094, 2019
65. Kishan AU, Lamb J, Casado M, et al: Magnetic resonance imaging-guided versus computed tomography-guided stereotactic body radiotherapy for prostate cancer (MIRAGE): Interim analysis of a phase III randomized trial. *J Clin Oncol* 40, 2022 (suppl 6; abstr 255)
66. Arya S, Das D, Engineer R, et al: Imaging in rectal cancer with emphasis on local staging with MRI. *Indian J Radiol Imaging* 25:148-161, 2015
67. Taylor FGM, Swift RL, Blomqvist L, et al: A systematic approach to the interpretation of preoperative staging MRI for rectal cancer. *AJR Am J Roentgenol* 191:1827-1835, 2008
68. Roberts LR, Sirlin CB, Zaiem F, et al: Imaging for the diagnosis of hepatocellular carcinoma: A systematic review and meta-analysis. *Hepatology* 67:401-421, 2018
69. Wald C, Russo MW, Heimbach JK, et al: New OPTN/UNOS policy for liver transplant allocation: Standardization of liver imaging, diagnosis, classification, and reporting of hepatocellular carcinoma. *Radiology* 266:376-382, 2013
70. Park M-S, Kim S, Patel J, et al: Hepatocellular carcinoma: Detection with diffusion-weighted versus contrast-enhanced magnetic resonance imaging in pretransplant patients. *Hepatology* 56:140-148, 2012
71. Voroney J-P, Brock KK, Eccles C, et al: Prospective comparison of computed tomography and magnetic resonance imaging for liver cancer delineation using deformable image registration. *Int J Radiat Oncol* 66:780-791, 2006
72. Pech M, Mohnike K, Wieners G, et al: Radiotherapy of liver metastases: Comparison of target volumes and dose-volume histograms employing CT- or MRI-based treatment planning. *Strahlenther Onkol* 184:256-261, 2008
73. Tan J, Lim Joon D, Fitt G, et al: The utility of multimodality imaging with CT and MRI in defining rectal tumour volumes for radiotherapy treatment planning: A pilot study. *J Med Imaging Radiat Oncol* 54:562-568, 2010
74. Couwenberg AM, Burbach JPM, Berbee M, et al: Efficacy of dose-escalated chemoradiation on complete tumor response in patients with locally advanced rectal cancer (RECTAL-BOOST): A phase 2 randomized controlled trial. *Int J Radiat Oncol* 108:1008-1018, 2020
75. Coolens C, Hawkins M, Ockwell C. Volume and motion definition in helical CT, 4DCT and MR imaging in upper gastrointestinal radiotherapy planning. Presented at 9th Biennial ESTRO Meeting, Barcelona, Spain, September 8–13, 2007
76. Heerkens HD, van Vulpen M, van den Berg CAT, et al: MRI-based tumor motion characterization and gating schemes for radiation therapy of pancreatic cancer. *Radiother Oncol* 111:252-257, 2014
77. Henke L, Kashani R, Robinson C, et al: Phase I trial of stereotactic MR-guided online adaptive radiation therapy (SMART) for the treatment of oligometastatic or unresectable primary malignancies of the abdomen. *Radiother Oncol* 126:519-526, 2018
78. de Jong EA, ten Berge JCEM, Dwarkasing RS, et al: The accuracy of MRI, endorectal ultrasonography, and computed tomography in predicting the response of locally advanced rectal cancer after preoperative therapy: A metaanalysis. *Surgery* 159:688-699, 2016
79. Lukovic J, Henke L, Gani C, et al: MRI-based upper abdominal organs-at-risk atlas for radiation oncology. *Int J Radiat Oncol* 106:743-753, 2020
80. Klüter S: Technical design and concept of a 0.35 T MR-Linac. *Clin Transl Radiat Oncol* 18:98-101, 2019
81. van der Valk MJM, Hilling DE, Bastiaannet E, et al: Long-term outcomes of clinical complete responders after neoadjuvant treatment for rectal cancer in the International Watch & Wait Database (IWWD): An international multicentre registry study. *The Lancet* 391:2537-2545, 2018
82. Fernandez LM, São Julião GP, Figueiredo NL, et al: Conditional recurrence-free survival of clinical complete responders managed by watch and wait after neoadjuvant chemoradiotherapy for rectal cancer in the International Watch & Wait Database: A retrospective, international, multicentre registry study. *Lancet Oncol* 22:43-50, 2021
83. Ladd ME, Bachert P, Meyerspeer M, et al: Pros and cons of ultra-high-field MRI/MRS for human application. *Prog Nucl Magn Reson Spectrosc* 109:1-50, 2018

84. Grant A, Metzger GJ, Van de Moortele P-F, et al: 10.5 T MRI static field effects on human cognitive, vestibular, and physiological function. *Magn Reson Imaging* 73:163-176, 2020
85. Lambin P, Leijenaar RTH, Deist TM, et al: Radiomics: The bridge between medical imaging and personalized medicine. *Nat Rev Clin Oncol* 14:749-762, 2017
86. Baumann M, Krause M, Overgaard J, et al: Radiation oncology in the era of precision medicine. *Nat Rev Cancer* 16:234-249, 2016
87. Winkel D, Bol GH, Kroon PS, et al: Adaptive radiotherapy: The Elekta Unity MR-linac concept. *Clin Transl Radiat Oncol* 18:54-59, 2019
88. Brock KK: Adaptive radiotherapy: Moving into the future. *Semin Radiat Oncol* 29:181-184, 2019
89. McCulloch P, Altman DG, Campbell WB, et al: No surgical innovation without evaluation: The IDEAL recommendations. *Lancet* 374:1105-1112, 2009
90. Verkooijen HM, Kerkmeijer LGW, Fuller CD, et al: R-IDEAL: A framework for systematic clinical evaluation of technical innovations in radiation oncology. *Front Oncol* 7:59, 2017
91. Elsherbini AAM, Saber M, Aggag M, et al: Magnetic nanoparticle-induced hyperthermia treatment under magnetic resonance imaging. *Magn Reson Imaging* 29:272-280, 2011
92. Meng Y, Pople CB, Lea-Banks H, et al: Safety and efficacy of focused ultrasound induced blood-brain barrier opening, an integrative review of animal and human studies. *J Control Release* 309:25-36, 2019
93. Thanou M, Gedroyc W: MRI-guided focused ultrasound as a new method of drug delivery. *J Drug Deliv* 2013:616197, 2013
94. McNabb E, Al-Mahrouki A, Law N, et al: Ultrasound-stimulated microbubble radiation enhancement of tumors: Single-dose and fractionated treatment evaluation. *PLoS One* 15:e0239456, 2020

